

The black M2-M5 ring intersection spins

Vasilis Niarchos^{*,†}

Crete Center for Theoretical Physics, Department of Physics, University of Crete, 71303, Greece.

E-mail: niarchos@physics.uoc.gr

Konstadinos Siampos[‡]

*Université de Mons-Hainaut (UMH), Place du Parc, 20, B-7000 Mons, Belgium.
CPHT – Ecole Polytechnique, CNRS UMR 7644, 91128 Palaiseau Cedex, France.*

E-mail: konstantinos.siampos@umons.ac.be

We review the blackfold description of the fully localized orthogonal M2-M5 intersection in eleven-dimensional supergravity which constitutes the direct gravitational analogue of the Howe-Lambert-West self-dual string soliton solution. We emphasize the preliminary implications of this description for the physics of the M2-M5 system and the novel research directions that it opens. This report contains several new results. As an extension of previous work we report new results on deformations of the M2-M5-KKW intersection that describe self-dual ring intersections. Extremal non-supersymmetric configurations of this type probe novel aspects of the M2-M5 system and allow us to explore further the merits and limitations of the blackfold description of black brane intersections. In particular, we provide an example of a situation where an effective description of extremal *non-supersymmetric* spike configurations is shown to capture correctly features of the exact solutions beyond its strict regime of validity. This observation hints at the existence of improved convergence properties in the underlying derivative expansion scheme without the necessary presence of supersymmetry.

Proceedings of the Corfu Summer Institute 2012 "School and Workshops on Elementary Particle Physics and Gravity"

September 8-27, 2012

Corfu, Greece

*Speaker.

†CCTP-2013-02

‡CPHT-RR027.0612

1. Effective descriptions of the orthogonal M2-M5 intersection

It is widely believed that much can be learned about the structure of M-theory and the non-perturbative structure of string theory by studying the properties of the theories that reside on M2 and M5 branes. In recent years considerable progress has been achieved by identifying the low-energy theory on M2 branes as an appropriately supersymmetric Chern-Simons-Matter theory [1–3]. Our understanding of the corresponding question for M5 branes is more rudimentary and currently the subject of active research.

Since M2 branes can end on M5 branes it has long been suspected that the theory that resides on M5 branes is a mysterious novel theory of non-critical strings. These strings are charged under the self-dual three-form field on the M5 brane—hence the usual reference to them as self-dual strings. Aspects of this theory are implicit in the orthogonal M2-M5 intersection

$$\begin{array}{cccccccccccc}
 & 0 & 1 & 2 & 3 & 4 & 5 & 6 & 7 & 8 & 9 & 10 \\
 \text{M2 :} & \bullet & \bullet & & & & & \bullet & & & & \\
 \text{M5 :} & \bullet & \bullet & \bullet & \bullet & \bullet & \bullet & & & & &
 \end{array} \tag{1.1}$$

The low-energy theory at the intersection is a two-dimensional field theory with large $\mathcal{N} = (4, 4)$ superconformal symmetry. It is desirable to identify the precise properties of this theory, for example, its central charge c as a function of the number N_2 of M2 branes and N_5 of M5 branes. Assuming unitarity the restrictive nature of the large $\mathcal{N} = (4, 4)$ superconformal algebra [4] dictates that there are two integers k_+ and k_- in terms of which

$$c = \frac{6k_+k_-}{k_+ + k_-} . \tag{1.2}$$

It is currently unknown how k_+ and k_- relate to N_2 and N_5 .

The existence of a gravitational solution in eleven-dimensional supergravity that describes the above 1/4-BPS intersection implies that there is a dual holographic description of the above superconformal field theory (SCFT) in terms of gravity on an appropriately warped $AdS_3 \times S^3 \times S^3 \times \mathcal{M}_2$ background with fluxes whose strength is related to the integers k_+ , k_- . The precise form of this solution in supergravity is also unknown. More generally, the holographic correspondence for two-dimensional SCFTs with large $\mathcal{N} = (4, 4)$ superconformal symmetry is an interesting but largely open subject (see [5, 6] and references therein for related previous work).

1.1 Howe-Lambert-West: an effective non-gravitational description

One of the first successful descriptions of the intersection (1.1) was given by Howe, Lambert and West in [7] using the effective fivebrane worldvolume theory of a single M5 brane [8–10]. In this language, a supersymmetric soliton solution describes how the orthogonal stack of M2 branes deforms the fivebrane worldvolume. The solution, which preserves the requisite $SO(1, 1) \times SO(4) \times SO(4)$ symmetry, has a non-trivial worldvolume self-dual three-form flux and a non-trivial transverse scalar field $z = x^6$ with the profile

$$z(\sigma) = \frac{2Q_{sd}}{\sigma^2} . \tag{1.3}$$

σ denotes the radial distance in the directions (2345) transverse to the self-dual string along the fivebrane worldvolume. Q_{sd} , which is proportional to the number of M2 branes N_2 , denotes the self-dual electric/magnetic charge of the self-dual string.

This solution is an M-theory analogue of the BIon solution in string theory [11] that describes how strings end on D-branes. It is also a nice illustration of the power of effective descriptions in string/M-theory. Although effective actions are only restricted to the description of slowly-varying configurations, they frequently allow us to go much further and capture non-trivial features of the theory bypassing the absence (in most cases) of a precise knowledge of the underlying microscopics.

In the case of the Howe, Lambert and West solution, the above effective description is known currently only for the case of a *single* M5 brane and an arbitrary finite number of M2 branes. The analogous description for a general number N_5 of M5 branes requires knowledge of the non-abelian structure of the effective M5 brane worldvolume theory, which is another interesting open problem.

1.2 Blackfold funnels: an effective gravitational description

Supergravity provides a complementary holographic description of the system in the deep non-abelian regime. The main technical issue in this approach is the complexity of the corresponding black brane intersection. There has been considerable work in this direction (see for instance [12–15]), with the state-of-the-art reported in [16], but the exact fully localized 1/4-BPS supergravity solution remains unknown. Non-extremal solutions are even harder to get and even further away from the reach of the currently known exact solution generating techniques.

Once again effective descriptions can sidestep the complexity of the exact equations and provide a useful new guide to the underlying physics. In the case at hand, we would be looking for an effective treatment of black brane solutions in supergravity that describe appropriately small deformations of the *planar* M2-M5 bound state black brane solution. The latter is an exactly known supergravity solution (see eqs. (2.1)-(2.5) below) that describes a stack of planar M5 branes with dissolved M2 brane charge. The deformations of interest would describe how a black M2 brane solution emerges orthogonally from such a fivebrane to form the direct gravitational analogue of the self-dual string soliton of [7]. The blackfold formalism [17–19], which provides a general effective worldvolume description of black brane dynamics, is perfectly suited for this task. In the case of the fully localized black M2-M5 intersection, blackfolds allow to replace the complicated system of partial differential equations of the exact supergravity equations of motion with a simpler effective fivebrane worldvolume description, which is part of a derivative expansion scheme. This is both conceptually and computationally attractive and makes a direct comparison with the abelian non-gravitational self-dual string soliton solution of [7] much more transparent.

The details of this description for the fully localized black M2-M5 intersection were provided recently in [20, 21]. The precise technical issues involved in this exercise will be explained in greater detail below for an interesting new extension that involves stationary M2-M5-KKW intersections. In the rest of this introduction we proceed to highlight the main results and physical implications of the recent work [20, 21].

A novel expansion. The blackfold description of the M2-M5 intersection is based on a derivative expansion scheme. As a description of a supergravity solution it is applicable in a large- N limit

where $N_2, N_5 \gg 1$. The formalism picks out naturally two dimensionful parameters to characterize the system

$$q_2 \propto GQ_2, \quad q_5 \propto GQ_5 \quad (1.4)$$

where G is the eleven-dimensional gravitational constant and Q_2, Q_5 the M2 and M5 charge densities respectively (see eqs. (2.16) for the precise definitions).¹ The perturbative expansion that organizes the blackfold description of the intersection is controlled by the unique dimensionless ratio of the parameters (1.4)

$$\frac{1}{\lambda} := \left| \frac{q_2}{q_5^2} \right| = \frac{4N_2}{N_5^2}. \quad (1.5)$$

This ratio controls how strongly the orthogonal M2s bend the fivebrane worldvolume. The derivative corrections are suppressed when λ is large. Already at this level this picture suggests something non-trivial about the $d = 2$ SCFT at the intersection. It suggests that it admits a corresponding large- N 't Hooft-like expansion where the integers N_2, N_5 are scaled to infinity with the ratio λ kept fixed. How this expansion arises in quantum field theory terms is an interesting open question.

Supersymmetric funnels. The effective fivebrane worldvolume theory of the black M2-M5 system involves (among other things) a set of five transverse scalars; the same set that describes the transverse space fluctuations of a fivebrane in the non-gravitational description. Specializing to extremal static configurations Ref. [20] showed that there is a non-trivial solution where a single scalar field $z = x^6$ is turned on and behaves as

$$z(\sigma) = 2\pi \frac{N_2}{N_5} \frac{\ell_P^3}{\sigma^2} \quad (1.6)$$

in direct analogy to the non-gravitational result (1.3), where ℓ_P is the eleven-dimensional Planck length scale. This spike solution is a three-sphere funnel electrically and magnetically charged under the three-form potential C_3 of eleven-dimensional supergravity. When extrapolated to the deep core at $\sigma = 0$ it captures correctly the *exact* tension and charge of an extremal black M2 brane solution.

This agreement with exact expectations here is at first sight rather impressive and miraculous. At $\sigma = 0$ the solution of the leading order equations of the effective description (that led to (1.6)) are developing very large gradients and lie well outside their strict regime of validity. The fact that the exact features of the emerging M2 are reproduced correctly hints that the convergence of the underlying expansion scheme of the effective description is much better than naively expected. This fact has also been stressed in the context of non-gravitational effective actions, most notably the case of the BIon solution [11] based on the use of the Dirac-Born-Infeld action. It is believed that the underlying reason for this improved behavior is supersymmetry. In the following sections, we will discover a new example where a similar observation extends beyond supersymmetry to extremal non-supersymmetric configurations. It appears that extremality (without necessarily supersymmetry) is enough to guarantee better convergence properties of the effective descriptions at hand. This is clearly an issue of general interest that deserves further study. In the ensuing, we rely

¹A related fact is that the near-horizon AdS_7 radius for a stack of M5 branes is $R_{AdS_7} = 2|q_5|^{\frac{1}{3}}$ and the near-horizon AdS_4 radius for a stack of M2 branes is $R_{AdS_4} = |q_2|^{\frac{1}{6}}/\sqrt{2}$.

on these improved convergence properties to motivate any further results based on leading order effective descriptions.

Near-extremal funnels and central charge scalings. Further information about the microscopic properties of the M2-M5 system can be obtained by studying the near-extremal thermodynamics of the supergravity solutions. The near-extremal behavior of the entropy is expected to be dominated by the infrared dynamics of the $d = 2$ SCFT at the intersection, and accordingly should behave at leading order in the small temperature limit in agreement with the Cardy formula as

$$s = \frac{\pi c}{6} T, \quad (1.7)$$

where s is the entropy density and c the central charge of the $d = 2$ SCFT at the intersection.

In Ref. [21] we studied the thermal version of the spike (1.6) and computed its near-extremal entropy. The leading order behavior in the small temperature limit behaves in accordance to equation (1.7) and when written in terms of N_2 and λ , or N_5 and λ , it yields

$$c \sim 0.04 \frac{N_2^{\frac{3}{2}}}{\sqrt{\lambda}} + \dots \sim 0.3 \frac{N_5^3}{\lambda^2} + \dots \quad (1.8)$$

The dots indicate subleading terms in negative powers of N_2 and N_5 respectively, and negative powers of the dimensionless ratio λ . The approximations and assumptions that go into the derivation of this result will be discussed in more detail within a more general system in the following sections.

There are three key features of the leading order formulae (1.8): the power of N_2 or N_5 , the power of λ , and the overall numerical coefficient. The power of N_2 or N_5 is the most robust feature of the result because it follows simply from dimensional analysis. The general Bekenstein-Hawking formula from gravity takes at leading order in the temperature expansion the form

$$s = \frac{C(q_2, q_5) T}{G} \quad (1.9)$$

where C is a constant that depends only q_2 and q_5 and has length dimension nine. Hence, when expressed in terms of N_2 and λ , or in terms of N_5 and λ the power of N_2 or N_5 is completely fixed as in (1.8). At the same time this feature makes a direct connection with the $N_2^{\frac{3}{2}}$ scaling of the degrees of freedom of M2 branes and the corresponding N_5^3 scaling of the M5 brane degrees of freedom and is therefore highly suggestive of the ‘dual’ M2 or M5 brane origin of the two-dimensional theory at the intersection.

The second feature, namely the precise power of the dimensionless ratio λ , cannot be fixed by dimensional analysis and is therefore a specific result of the blackfold calculation. Assuming the basic premises of the computation we do not expect higher order terms to change this result. The third feature on the other hand, *i.e.* the overall numerical coefficient, is not robust and it is not unreasonable to expect that it changes in a more exact treatment of the system.

Finally, it is natural to ask how (1.8) compares with the exact formula (1.2). When expressed in terms of N_2, N_5 eq. (1.8) takes the form

$$c \sim 0.6 \frac{N_2^2}{N_5} + \dots \quad (1.10)$$

Both (1.2) and (1.10) are roughly speaking a ratio of the product of two integers over another integer, but without a more detailed knowledge about the precise relation between k_+, k_- and N_2, N_5 it is impossible to decide conclusively if the results are indeed compatible. This and other features of the above results raise a number of interesting questions that require further study. We shall discuss them further in the concluding section.

2. The M2-M5 blackfold toolkit

The blackfold formalism provides a general effective worldvolume description of the long-wavelength dynamics of black branes. A detailed introduction to the formalism can be found in the original work [17–19] and the reviews [22, 23]. For some of the previous applications of the formalism to black hole physics and string theory we refer the reader to [24–29] and references therein. Static configurations of the M2-M5 intersection were treated recently in this framework in [20, 21]. In what follows we will extend the analysis of [20, 21] to stationary M2-M5-KKW configurations by adding rotation in the direction of the intersection. Here we review the pertinent equations of the formalism and set up our notation.

The M2-M5 blackfold equations describe the long-wavelength dynamics of the black M2-M5 bound state [30–34]

$$ds_{11}^2 = (HD)^{-1/3} \left[-f dt^2 + (dx^1)^2 + (dx^2)^2 + D((dx^3)^2 + (dx^4)^2 + (dx^5)^2) + H(f^{-1} dr^2 + r^2 d\Omega_4^2) \right], \quad (2.1)$$

$$C_3 = -\sin \theta (H^{-1} - 1) \coth \alpha dt \wedge dx^1 \wedge dx^2 + \tan \theta DH^{-1} dx^3 \wedge dx^4 \wedge dx^5, \quad (2.2)$$

$$C_6 = \cos \theta D(H^{-1} - 1) \coth \alpha dt \wedge dx^1 \wedge \cdots \wedge dx^5, \quad (2.3)$$

$$F_4 = dC_3 + \star_{11} dC_6, \quad (2.4)$$

$$H = 1 + \frac{r_0^3 \sinh^2 \alpha}{r^3}, \quad f = 1 - \frac{r_0^3}{r^3}, \quad D^{-1} = \cos^2 \theta + \sin^2 \theta H^{-1}. \quad (2.5)$$

The above exact solution of the supergravity equations describes a planar black fivebrane with M2 brane charge dissolved in its worldvolume along the (012) plane. The solution is parameterized by the constants r_0 , α and θ which control the temperature, the M2 and the M5 brane charge. Angular momentum along the fivebrane directions can be added with a general boost transformation. This transformation introduces a unit-norm velocity six-vector with components u^a . A boost along the intersection describes the black M2-M5-KKW solution [35, 31, 36].

The basic thermodynamic data of the solution (2.1)-(2.5) are captured by the following quantities [33]

$$\varepsilon = \frac{\Omega_{(4)}}{16\pi G} r_0^3 (1 + 3 \cosh^2 \alpha), \quad \mathcal{T} = \frac{3}{4\pi r_0 \cosh \alpha}, \quad s = \frac{\Omega_{(4)}}{4G} r_0^4 \cosh \alpha, \quad (2.6)$$

$$Q_5 = \cos \theta Q, \quad \mathbb{Q}_2 = -\sin \theta Q, \quad Q = \frac{\Omega_{(4)}}{16\pi G} 3r_0^3 \sinh \alpha \cosh \alpha, \quad (2.7)$$

$$\Phi_5 = \cos \theta \Phi, \quad \Phi_2 = -\sin \theta \Phi, \quad \Phi = \tanh \alpha. \quad (2.8)$$

ε denotes the energy density, \mathcal{T} the temperature, s the entropy density, Q_5 the fivebrane charge, \mathbb{Q}_2 the twobrane charge density, and Φ_5, Φ_2 the corresponding chemical potentials. We shall reserve

the notation Q for charges and \mathbb{Q} for charge densities. In this notation $\mathbb{Q}_5 = Q_5$. The free energy of the solution is

$$\mathcal{F} = \varepsilon - \mathcal{F}_s = \frac{\Omega_{(4)}}{16\pi G} r_0^3 (1 + 3 \sinh^2 \alpha) . \quad (2.9)$$

$\Omega_{(n)} = \frac{2\pi^{\frac{n+1}{2}}}{\Gamma(\frac{n+1}{2})}$ denotes the volume of the unit round n -sphere.

In analogy to standard treatments of D-branes in string theory we want to describe long-wavelength deformations of this solution. For example, we want to describe how one spins and bends the planar bound state (2.1)-(2.5). This is achieved with an effective hydrodynamic world-volume theory that describes the dynamics of an effective fluid on a dynamical fivebrane world-volume. The relevant parameters of this theory are the variables r_0, α, θ, u^a (which become local functions of the coordinates of the effective fivebrane worldvolume) with the addition of five transverse scalars that capture the bending of the fivebrane in its eleven-dimensional ambient space and a unit three-form that keeps track of the local M2 brane current and its distribution inside the fivebrane worldvolume. As in the fluid-gravity correspondence [37, 38], there is in principle a one-to-one map between the solutions of this effective theory and specific supergravity solutions. In what follows, we will describe only the solutions of the effective theory. The precise map to bulk supergravity solutions is an open problem and the subject of on-going work (see section 6 for further comments).

The relevant equations of motion of the effective theory at leading order in the derivative expansion can be summarized as follows.

2.1 Leading order equations of motion

The equations of motion are split naturally to *intrinsic equations* that refer to fluctuations parallel to the worldvolume directions, and *extrinsic equations* that refer to fluctuations transverse to the worldvolume directions. The former constitute the hydrodynamic component of the dynamics, which is also familiar from the fluid-gravity correspondence. The latter are the component that resembles more closely the dynamics familiar from D-branes in string theory, which is usually captured by the Dirac-Born-Infeld action (or its analogue for M-branes).

Intrinsic equations. The intrinsic equations are conservation equations for the stress-energy momentum tensor and the M2, M5 brane currents

$$D_a T^{ab} = 0 \quad (2.10)$$

$$d \star_6 J_3 = 0 , \quad J_3 = \mathbb{Q}_2 \hat{V}_{(3)} , \quad (2.11)$$

$$d \star_6 J_6 = 0 , \quad J_6 = Q_5 \hat{V}_{(6)} . \quad (2.12)$$

We use latin letters $a, b, \dots = 0, 1, \dots, 5$ to denote the worldvolume coordinates.

The derivative D_a is the covariant derivative with respect to the induced worldvolume metric γ_{ab} . T_{ab} is the stress-energy tensor

$$T_{ab} = \mathcal{F}_s \left(u_a u_b - \frac{1}{3} \gamma_{ab} \right) - \Phi_2 \mathbb{Q}_2 \hat{h}_{ab} - \Phi_5 Q_5 \gamma_{ab} , \quad (2.13)$$

which is derived from the thermodynamics of the planar solution (2.6) with a general boost transformation. The relevant parameters, $r_0, \alpha, \text{etc.}$, have been promoted to local functions of the

worldvolume coordinates $\hat{\sigma}^a$ ($a = 0, 1, \dots, 5$). \hat{h}_{ab} is a projector along the worldvolume directions of the dissolved M2 brane. In the special case of (2.1)-(2.5) \hat{h}_{ab} projects along the plane (012). In more general configurations, \hat{h}_{ab} needs to be determined by solving the equations of motion.

In the charge conservation equations (2.11), (2.12) $\hat{V}_{(3)}$ denotes a unit volume 3-form along the directions of the M2 brane current and $\hat{V}_{(6)}$ the unit volume form of the fivebrane worldvolume. The six-current equation (2.12) implies trivially

$$\partial_a Q_5 = 0 \quad (2.14)$$

from which we can deduce that Q_5 is an overall constant that participates passively in the dynamics. The M2 brane charge density and its distribution inside the fivebrane worldvolume, however, are dynamical quantities controlled by (2.10), (2.11).

In terms of the number of M2 and M5 branes, N_2, N_5 respectively,

$$Q_2 = \frac{N_2}{(2\pi)^2 \ell_P^3}, \quad Q_5 = \frac{N_5}{(2\pi)^5 \ell_P^6}. \quad (2.15)$$

As already advertised it will also be useful to introduce the rescaled versions of the charges

$$q_2 = -\frac{16\pi G}{3\Omega_{(3)}\Omega_{(4)}} Q_2 = -4\pi^2 N_2 \ell_P^6, \quad q_5 = \frac{16\pi G}{3\Omega_{(4)}} Q_5 = \pi N_5 \ell_P^3. \quad (2.16)$$

The minus sign in the definition of q_2 is a convention.

Extrinsic equations. The extrinsic equations can be recast into the form [39]

$$K_{ab}{}^\mu T^{ab} = 0 \quad (2.17)$$

where $K_{ab}{}^\mu$ is the extrinsic curvature tensor [18]. For the system of interest in this work explicit formulae for all the components of $K_{ab}{}^\mu$ appear in appendix B.

In the following sections we solve the above system of equations to determine the complete profile of stationary configurations that describe rotating M2 branes ending on M5 branes.

2.2 Thermodynamics

Stationary solutions entail a Killing vector ξ that defines unit-time translations at the asymptotic infinity and a spacelike Killing vector χ that generates rotations. We assume that the vector ξ on the six-dimensional worldvolume \mathscr{W}_6 is orthogonal to spacelike hypersurfaces \mathscr{B}_5 and define the unit normal

$$n^a = \frac{1}{R_0} \xi^a \Big|_{\mathscr{W}_6}. \quad (2.18)$$

The factor R_0 measures the local gravitational redshift between points on \mathscr{W}_6 and the asymptotic infinity. In our case this factor will be trivial, namely $R_0 = 1$, but it can be non-trivial in other cases of interest, *e.g.* for blackfolds in AdS backgrounds [40, 41].

Once we have a complete stationary solution of the equations described in the previous subsection the leading order thermodynamics of the supergravity solution can be determined straightforwardly with the use of the following general expressions for the mass, angular momentum and entropy [18]

$$M = \int_{\mathscr{B}_5} dV_{(5)} T_{ab} n^a \xi^b, \quad J = - \int_{\mathscr{B}_5} dV_{(5)} T_{ab} n^a \chi^b, \quad S = - \int_{\mathscr{B}_5} dV_{(5)} s u_a n^a. \quad (2.19)$$

We shall compute these quantities in specific cases in the following sections.

3. M2-M5-KKW ring intersections

In previous work [20, 21] we analyzed the static configuration (1.1) with symmetry group $SO(1,1)_{01} \times SO(4)_{2345} \times SO(4)_{789(10)}$ (the subscripts refer to the planes rotated by the corresponding symmetry group). In this case the intersection is an infinite open string. In what follows we extend the analysis to describe a configuration that realizes a closed string intersection. A simple option, that preserves the same symmetry group as above, is to compactify the direction x^1 of the ambient spacetime. This is a trivial choice that will not add anything particularly new to the analysis of [20].

However, qualitatively new configurations on the flat eleven-dimensional Minkowski background arise by bending the extrinsic geometry of the M2 and M5 branes. We shall be looking for configurations that arise from the intersection of a cylindrical black M2 brane with a black M5 brane. A cylindrical black M2 brane is not a regular stationary configuration unless it has non-zero angular momentum to balance the gravitational attraction.² In this way, we are naturally led to the discussion of a deformation of the M2-M5-KKW intersection that describes rotating cylindrical M2s ending orthogonally on M5s along a rotating self-dual ring. Such configurations preserve a smaller symmetry group, at most $SO(1,1) \times SO(4) \times SO(3)$.

3.1 Two candidate stationary configurations that fail

Cylindrical M2 on a planar M5. We are asking if there is a fully localized supergravity solution that describes the orthogonal intersection of a rotating cylindrical black M2 brane along the directions $(0\vartheta 6)$ with a planar black M5 brane along the plane (012345) . The spatial part of the intersection is a circle along the angular direction ϑ inside the 2-plane (12). The answer to this question is negative in the blackfold approximation for the following reason.

Let us parametrize the ambient eleven-dimensional Minkowski metric as

$$ds_{11}^2 = -dt^2 + d\rho^2 + \rho^2 d\vartheta^2 + dr^2 + r^2(d\psi^2 + \sin^2\psi d\varphi^2) + \sum_{i=6}^{10} (dx^i)^2. \quad (3.1)$$

We have expressed the 2-plane (12) in terms of the polar coordinates (ρ, ϑ) and the transverse \mathbb{R}^3 on the fivebrane worldvolume in spherical coordinates (r, ψ, φ) . Then, the embedding of interest is described by the ansatz

$$\begin{aligned} t(\hat{\sigma}^a) &= \hat{\sigma}^0, \quad \rho(\hat{\sigma}^a) = \hat{\sigma}^1, \quad \vartheta(\hat{\sigma}^a) = \hat{\sigma}^2, \quad r(\hat{\sigma}^a) = \hat{\sigma}^3, \quad \psi(\hat{\sigma}^a) = \hat{\sigma}^4, \quad \varphi(\hat{\sigma}^a) = \hat{\sigma}^5, \\ x^6(\hat{\sigma}^a) &:= z(r, \rho), \quad x^i = 0 \quad (i = 7, 8, 9, 10). \end{aligned} \quad (3.2)$$

We activate only one of the transverse scalars, x^6 , which is a function of both $(\hat{\sigma}^1, \hat{\sigma}^3) = (\rho, r)$.

We are searching for a stationary solution of the equations (2.10)-(2.12), (2.17) with angular momentum along the direction ϑ . For such solutions the worldvolume velocity field u^a takes the form [18]

$$u = \frac{\xi + \Omega\chi}{|\xi + \Omega\chi|} = \frac{1}{\sqrt{1 - \Omega^2\rho^2}} \left(\frac{\partial}{\partial t} + \Omega \frac{\partial}{\partial \vartheta} \right) \quad (3.3)$$

²Appendix A summarizes the main features of the blackfold description of rotating black M2 cylinders.

where $\xi = \frac{\partial}{\partial t}$, $\chi = \frac{\partial}{\partial \vartheta}$ are the Killing vectors of time translation and rotation of the previous section 2.2. Ω is a the constant angular velocity of the configuration.

In order to have a solution with a well-defined real velocity field u the worldvolume coordinate $\hat{\sigma}^1 = \rho$ must be bounded from above and be less than $1/\Omega$. This implies that the M5 worldvolume is a disc in the (12) plane and cannot extend to $\rho = +\infty$. This configuration contradicts the conservation equation (2.14). Hence, we conclude that the ansatz (3.2) cannot satisfy the blackfold equations excluding M2-M5 black brane intersections of this form.

Cylindrical M2 on a spherical M5. We can try to amend the flaws of the above configuration by compactifying the M5 brane worldvolume on a five-sphere. Using spherical coordinates we can parametrize the ambient eleven-dimensional Minkowski metric as

$$\begin{aligned} ds_{11}^2 &= -dt^2 + dr^2 + r^2 d\Omega_5^2 + (dx^6)^2 + \sum_{j=8}^{10} (dx^j)^2, \\ d\Omega_5^2 &= d\varphi^2 + \sin^2 \varphi d\theta^2 + \sum_{i=1}^3 \mu_i(\varphi, \theta)^2 d\phi_i^2. \end{aligned} \quad (3.4)$$

The angles $\varphi, \theta \in [0, \frac{\pi}{2})$, μ_i are three directional cosines³ and $\phi_i \in [0, 2\pi)$ are three Cartan angles that parametrize the round five-sphere. We are using spherical coordinates for the plane (123457) where the fivebrane has co-dimension one. The ansatz of interest is

$$\begin{aligned} t(\hat{\sigma}^a) &= \hat{\sigma}^0, \quad \phi_i(\hat{\sigma}^a) = \hat{\sigma}^i \quad (i = 1, 2, 3), \quad \varphi(\hat{\sigma}^a) = \hat{\sigma}^4, \quad \theta(\hat{\sigma}^a) = \hat{\sigma}^5, \quad r(\hat{\sigma}^a) = r(\varphi), \\ x^6(\hat{\sigma}^a) &:= z(\varphi), \quad x^i = 0 \quad (i = 8, 9, 10) \end{aligned} \quad (3.5)$$

and the fluid velocity can be taken in general to be proportional to the vector

$$\frac{\partial}{\partial t} + \Omega_1 \frac{\partial}{\partial \phi_1} + \Omega_2 \frac{\partial}{\partial \phi_2} + \Omega_3 \frac{\partial}{\partial \phi_3}, \quad (3.6)$$

where Ω_i ($i = 1, 2, 3$) are constant angular velocities. The intersection lies along a linear combination of the Cartan angles.

With this ansatz one can run again the formalism to find solutions. There is no a priori sign in the formalism that prevents the existence of such solutions, yet in all cases that we examined⁴ the resulting solutions were found to be singular. Although we have not proven that all pertinent solutions of the above type are singular there are reasons to believe that this is the case. Microscopic configurations where a stack of M2s ends on a spherical M5 are essentially disallowed by the Gauss law, *i.e.* the fact that the flux of the self-dual three-form field has nowhere to go on a five-sphere. It is natural to expect that the absence of analogous regular configurations in the blackfold formalism is gravity's way of disallowing such configurations.

3.2 Rotating M2-M5 cylinders

A third option is to have a cylindrical black M2 end on a cylindrical black M5. This involves the following choice of coordinates and ansatz. We parametrize the ambient eleven-dimensional

³In terms of φ, θ : $\mu_1 = \cos \theta \sin \varphi$, $\mu_2 = \sin \theta \sin \varphi$, $\mu_3 = \cos \varphi$.

⁴The simplest most symmetric configurations that can be explored have equal angular velocities $\Omega_1 = \Omega_2 = \Omega_3$.

Minkowski metric as

$$ds_{11}^2 = -dt^2 + \rho^2 d\vartheta^2 + dr^2 + r^2(d\psi^2 + \sin^2\psi(d\phi^2 + \sin^2\phi d\omega^2)) + d\rho^2 + (dx^6)^2 + \sum_{i=8}^{10} (dx^i)^2 \quad (3.7)$$

and make the ansatz

$$\begin{aligned} t(\hat{\sigma}^a) &= \hat{\sigma}^0, \quad \vartheta(\hat{\sigma}^a) = \hat{\sigma}^1, \quad r(\hat{\sigma}^a) = \hat{\sigma}^2 := \sigma, \quad \psi(\hat{\sigma}^a) = \hat{\sigma}^3, \quad \phi(\hat{\sigma}^a) = \hat{\sigma}^4, \quad \omega(\hat{\sigma}^a) = \hat{\sigma}^5 \\ \rho(\hat{\sigma}^a) &= \rho(\sigma), \quad x^6(\hat{\sigma}^a) := z(\sigma), \quad x^i = 0 \quad (i = 8, 9, 10). \end{aligned} \quad (3.8)$$

We are using polar coordinates (ρ, ϑ) for the plane (17) where the fivebrane worldvolume has co-dimension one. The angles (ψ, ϕ, ω) parametrize a round three-sphere. Compared to the ansatz (3.2) that involved the activation of a single transverse scalar $z(r, \rho)$, here we are activating two transverse scalars $\rho(\sigma), z(\sigma)$, which are functions of a single worldvolume coordinate. The velocity field takes the same form as in eq. (3.3).

There are non-trivial solutions based on the ansatz (3.8). We shall discuss them in much detail in sections 4 and 5.

3.3 Characteristic scales

The configurations of subsection 3.2 possess four characteristic scales: (a) the transverse size of the black brane geometry (2.1) which is controlled by the charge radius [27, 26]

$$r_c(\sigma) := r_0(\sigma)(\sinh \alpha(\sigma) \cosh \alpha(\sigma))^{\frac{1}{3}}, \quad (3.9)$$

(b) the S^3 radius σ of the induced geometry, and (c) two characteristic length sizes, $L_{\text{curv}}^{(z)}, L_{\text{curv}}^{(\rho)}$, of the extrinsic curvature defined in appendix B. The perturbative blackfold expansion scheme is based on the hierarchy [18, 27, 26]

$$r_c(\sigma) \ll \min\left(\sigma, L_{\text{curv}}^{(z)}, L_{\text{curv}}^{(\rho)}\right). \quad (3.10)$$

Near extremality the leading behavior of these scales is set by the extremal solution that will be analyzed in the next section. In that case the precise regime implied by the inequalities in (3.10) yields constraints that will be presented in subsection 4.2 below.

4. Extremal rotating spikes

It will be convenient to begin our survey of rotating spike solutions from the extremal, zero-temperature case. In our setup one can show that this involves an extremal limit of the blackfold equations with a null momentum wave along the direction ϑ of rotation. Such limits were studied in [19] and take the form

$$\sqrt{\mathcal{T}} su^a := \sqrt{\mathcal{K}} l^a, \quad \mathcal{T} \rightarrow 0, \quad l^a l_a = 0, \quad \mathcal{K} = \text{finite}. \quad (4.1)$$

The local temperature \mathcal{T} is scaled to zero while the velocity field u^a becomes null. \mathcal{K} denotes the null momentum density, which will be a worldvolume-dependent quantity to be determined by

solving the equations of motion. In this limit the stress-energy tensor T^{ab} that controls the blackfold equations becomes

$$T^{ab} = \mathcal{K} l^a l^b - \Phi_2 \mathbb{Q}_2 \hat{h}^{ab} - \Phi_5 \mathbb{Q}_5 \gamma^{ab} . \quad (4.2)$$

With the ansatz of subsection 3.2

$$l = \frac{\partial}{\partial t} + \Omega \frac{\partial}{\partial \theta} \quad (4.3)$$

and the velocity field (3.3) becomes null when

$$\rho = \frac{1}{\Omega} . \quad (4.4)$$

The induced metric γ_{ab} and the two-brane projector \hat{h}_{ab} take the form

$$\gamma = \text{diag} \left(-1, \rho^2, 1 + z'^2, \sigma^2, \sigma^2 \sin^2 \psi, \sigma^2 \sin^2 \psi \sin^2 \varphi \right) , \quad (4.5)$$

$$\hat{h} = \text{diag} \left(-1, \rho^2, 1 + z'^2, 0, 0, 0 \right) . \quad (4.6)$$

We shall be using the notation $' := \frac{d}{d\sigma}$.

4.1 The solution

We are solving the equations

$$K_{ab}{}^\mu T^{ab} = 0 , \quad (4.7)$$

$$D_a T^{ab} = 0 , \quad (4.8)$$

$$d \star_6 (\mathbb{Q}_2 \hat{V}_{(3)}) = 0 \quad (4.9)$$

for the unknown functions $z(\sigma)$, $\theta(\sigma)$, $\mathcal{K}(\sigma)$, $Q(\sigma)$. In the extremal limit we scale the variables r_0 , α to 0, ∞ respectively keeping the quantity Q in eq. (2.7) fixed. Consequently,

$$\Phi_2 = -\sin \theta , \quad \Phi_5 = \cos \theta , \quad \Phi = 1 . \quad (4.10)$$

The set of extrinsic equations (4.7) gives two independent equations (for explicit expressions of the extrinsic curvature tensor see (B.1) in appendix B)

$$\frac{z''}{z'(1+z'^2)} = -\frac{3 \cos^2 \theta}{\sigma} , \quad \mathcal{K} = Q \Rightarrow T^{11} = 0 . \quad (4.11)$$

The second equation reproduces the condition of vanishing tension familiar from previous studies of black ring solutions [42].

The intrinsic equations (4.8), (4.9) lead to two additional independent relations

$$\sigma \mathcal{K}' + 3 \sin^2 \theta \mathcal{K} = 0 , \quad (4.12)$$

$$(\sigma^3 \sin \theta \mathcal{K})' = 0 \quad (4.13)$$

where we made use of the second equation $\mathcal{K} = Q$ in (4.11). We solve both of them by setting

$$\cos \theta = \frac{1}{\sqrt{1 + \frac{\kappa^2}{\sigma^6}}}, \quad \mathcal{K} = Q = Q_5 \sqrt{1 + \frac{\kappa^2}{\sigma^6}}. \quad (4.14)$$

κ is a constant which is related to the total M2, M5 charges in the following way

$$\kappa = \frac{1}{2\pi^2} \frac{Q_2}{Q_5} = 4\pi \frac{N_2}{N_5} \ell_p^3. \quad (4.15)$$

The three-funnel profile $z(\sigma)$ is now fixed completely by the first equation in (4.11), which takes the same form as in the static case analyzed in [20]. With boundary conditions

$$\lim_{\sigma \rightarrow +\infty} z(\sigma) = 0, \quad \lim_{\sigma \rightarrow \sigma_0^+} z'(\sigma) = -\infty \quad (4.16)$$

we find

$$z(\sigma) = \frac{\sqrt{\sigma_0^6 + \kappa^2}}{2\sigma^2} {}_2F_1\left(\frac{1}{3}, \frac{1}{2}, \frac{4}{3}; \frac{\sigma_0^6}{\sigma^6}\right). \quad (4.17)$$

The spike solution that reproduces (1.6) has $\sigma_0 = 0$.

The above solutions are zero-temperature extremal configurations. For zero angular velocity, $\Omega = 0$, the radius ρ of the intersection becomes infinite and we recover the static solutions of [20],⁵ which are expected to be 1/4-BPS for $\sigma_0 = 0$. As was mentioned previously, the addition of angular momentum breaks some of the overall symmetry. As we discuss further in a moment we have good reasons to believe that it also breaks completely the supersymmetry. Hence, in the presence of non-zero angular momentum all of the above solutions are extremal but non-supersymmetric.

4.2 Validity of the leading order approximation

Near extremality the leading behavior of the characteristic scales $r_c, L_{\text{curv}}^{(z)}, L_{\text{curv}}^{(\rho)}$ (see subsection 3.3) is set by the extremal solution we have just presented. One can show, using the definitions and above expressions, or by taking the extremal limit of eqs. (5.7)-(5.8) below, that

$$r_c(\sigma) = q_5^{\frac{1}{3}} \left(1 + \frac{\kappa^2}{\sigma^6}\right)^{\frac{1}{6}} \quad (4.18)$$

with the constant κ defined in eq. (4.15) and q_5 the constant in eq. (2.16). The leading behavior of the characteristic curvature sizes $L_{\text{curv}}^{(z)}, L_{\text{curv}}^{(\rho)}$ can be determined with the use of the expressions in appendix B. We find

$$L_{\text{curv}}^{(z)} = \frac{\sigma(\sigma^6 + \kappa^2)^{\frac{3}{2}}}{3\kappa^2 \sqrt{\sigma_0^6 + \kappa^2}}, \quad L_{\text{curv}}^{(\rho)} = \frac{1}{\Omega}. \quad (4.19)$$

Moreover, it was argued in Ref. [21] that the perturbative corrections to the leading order result are controlled by negative powers of the ratio $\lambda = \frac{N_5^2}{4N_2}$. It will therefore be natural to work in the limit $\lambda \gg 1$ where these corrections are suppressed.

⁵The static solutions [20] have the same z profile as in (4.17).

Consequently, the first inequality in (3.10), $r_c(\sigma) \ll \sigma$, implies

$$\sigma \gg \sigma_c = \left(\frac{\pi N_5}{\sqrt{2}} \right)^{\frac{1}{3}} \left(1 + \sqrt{1 + \frac{64N_2^2}{N_5^4}} \right)^{\frac{1}{6}} \ell_P \quad (4.20)$$

where by definition σ_c is the point where $r_c(\sigma_c) = \sigma_c$. The second inequality, $r_c(\sigma) \ll L_{\text{curv}}^{(z)}$, is automatically satisfied given (4.20). The third inequality, $r_c(\sigma) \ll L_{\text{curv}}^{(\rho)}$, is satisfied only when

$$\sigma \gg \tilde{\sigma}_c := \frac{\Omega q_2^{\frac{1}{3}}}{(1 - \Omega^6 q_5^2)^{\frac{1}{6}}} . \quad (4.21)$$

We are assuming

$$\Omega < q_5^{-\frac{1}{3}} , \quad (4.22)$$

which places an upper bound on the angular velocity Ω . Since

$$\tilde{\sigma}_c \leq \left(\frac{\kappa}{2} \right)^{\frac{1}{3}} < \left(\frac{1}{\sqrt{2}\lambda} \right)^{\frac{1}{3}} \sigma_c \quad (4.23)$$

we deduce that the inequality (4.21) is automatically satisfied in the limit $\lambda \gg 1$ given (4.20).

We conclude that there is a characteristic lower bound scale $\sigma_c(N_2, N_5)$ on the radius σ below which the leading order blackfold description of the extremal fully localized M2-M5 intersection is beyond the strict regime of its validity. Any quantity computed below this scale cannot be trusted and is anticipated a priori to diverge considerably from the exact result. Interestingly, there are quantities for which such deviations are not observed.

4.3 Miraculous agreement beyond the strict regime of validity

The mass and angular momentum densities of the solution (4.17) can be determined straightforwardly from the general expressions (2.19). With a little algebra one finds

$$\frac{dM}{dz} = 2\Omega \frac{dJ}{dz} = \frac{4\pi\Omega_{(3)} \mathcal{H}}{\Omega} \frac{\sqrt{1+z'^2}}{z'} \sigma^3 = -\frac{4\pi Q_2}{\kappa\Omega} \frac{\kappa^2 + \sigma^6}{\sqrt{\kappa^2 + \sigma_0^6}} . \quad (4.24)$$

The entropy density of the extremal solutions is vanishing.

It is interesting to note the following property. The spike solutions have $\sigma_0 = 0$ and extend all the way to $z = +\infty$. At that point, namely the tip of the spike, the mass and angular momentum densities reproduce exactly the corresponding quantities of extremal cylindrical M2 black branes. Indeed, (4.24) gives

$$\left. \frac{dM}{dz} \right|_{\sigma=\sigma_0=0} = -\frac{4\pi Q_2}{\Omega} = T_{M_2} , \quad \left. \frac{dJ}{dz} \right|_{\sigma=\sigma_0=0} = -\frac{2\pi Q_2}{\Omega^2} = \mathcal{J}_{M_2} \quad (4.25)$$

where T_{M_2} and \mathcal{J}_{M_2} are respectively the tension and angular momentum density of an extremal cylindrical M2 black brane with the same charge (see eq. (A.15) in appendix A).

This matching is impressive because it occurs in a region ($\sigma \sim 0 \ll \sigma_c$) where the leading order blackfold approximation breaks down. The same impressive matching has been observed also in

the case of the F1-D3 BIon [27], and the case of the static M2-M5 intersection [20], generalizing in gravity the corresponding observations in the DBI treatment of the BIon [11]. In both cases the extremal intersection is supersymmetric making supersymmetry the natural candidate for the underlying reasons behind this miraculous matching. This matching is an indication that under suitable conditions, *e.g.* supersymmetry, effective treatments like the DBI, blackfolds *etc.* can enjoy much better convergence properties than naively anticipated on general grounds.

In the case at hand, however, the agreement (4.25) is even more impressive. Besides the fact that it involves the matching of two quantities (tension and angular momentum density), it occurs for a solution that is extremal but non-supersymmetric. Indeed, the solution describes a fivebrane that deforms to become in a region of spacetime a rotating cylindrical M2 black brane. Since a cylindrical M2 brane has only a dipole M2 charge, it is not expected to be supersymmetric [19]. This implies that the whole configuration is extremal but non-supersymmetric. Consequently, this is an interesting new example where the cancellations (and better convergence properties) implied by the above matching occur at extremality without the necessary presence of supersymmetry. Further related unexpected agreements will be noted for the near-extremal solutions in the next section.

5. Thermally excited rotating spikes

Further aspects of the system are revealed by studying it at non-zero temperature. For instance, near-extremal black brane thermodynamics is one way to derive information about the microscopic structure of the system [43], and this is how we arrived at the central charge expression (1.8) in Ref. [21] for the static $\Omega = 0$ intersection. In this section we proceed to analyze the near-extremal properties of the rotating spike solutions generalizing the discussion of Ref. [21]. One of the new features of the finite-temperature solutions is that ρ is no longer constrained by the extremality condition (4.4). Hence, both transverse scalars ρ and z are now non-trivial functions of the worldvolume coordinate σ and we have to solve a more complicated system of differential equations.

5.1 Equations of motion and general thermodynamic expressions

A finite-temperature configuration is obtained by solving the blackfold equations (4.7)-(4.9) for the unknown functions $z(\sigma)$, $\rho(\sigma)$, $r_0(\sigma)$, $\alpha(\sigma)$, $\theta(\sigma)$. The induced metric and two-brane projector \hat{h}_{ab} take the explicit form

$$\gamma = \text{diag} \left(-1, \rho^2, 1 + \rho'^2 + z'^2, \sigma^2, \sigma^2 \sin^2 \psi, \sigma^2 \sin^2 \psi \sin^2 \varphi \right), \quad (5.1)$$

$$\hat{h} = \text{diag} \left(-1, \rho^2, 1 + z'^2 + \rho'^2, 0, 0, 0 \right). \quad (5.2)$$

Since we are looking for stationary solutions the velocity field is oriented along a Killing vector

$$u = \frac{1}{\sqrt{1 - \Omega^2 \rho^2}} \left(\frac{\partial}{\partial t} + \Omega \frac{\partial}{\partial \vartheta} \right) \quad (5.3)$$

and the intrinsic equations are satisfied by requiring that the following quantities [20, 21]

$$q_2 = -\frac{16\pi G}{3\Omega_{(3)}\Omega_{(4)}} Q_2 = \sigma^3 r_0^3 \sin \theta \sinh \alpha \cosh \alpha, \quad (5.4)$$

$$q_5 = \frac{16\pi G}{3\Omega_{(4)}} Q_5 = r_0^3 \cos \theta \sinh \alpha \cosh \alpha , \quad (5.5)$$

$$\frac{r_0 \cosh \alpha}{\sqrt{1 - \Omega^2 \rho^2}} = \beta := \frac{3}{4\pi T} . \quad (5.6)$$

are σ -independent constants. q_2, q_5 are the same rescaled versions of the total charges Q_2, Q_5 as in eq. (2.16), while T expresses the global temperature of the solution. This leaves the extrinsic equations that determine the profile of the transverse scalars z, ρ , which will be discussed momentarily.

Solving the above equations for the unknowns α, θ, r_0 we find, as in [20], two solutions (denoted by the subscript \pm)

$$\cosh \alpha_{\pm} = \frac{\beta^3}{\sqrt{2}q_5} (1 - \Omega^2 \rho^2)^{\frac{3}{2}} \frac{\sqrt{1 \pm \sqrt{1 - \frac{4q_5^2}{\beta^6} \left(1 + \frac{\kappa^2}{\sigma^6}\right) (1 - \Omega^2 \rho^2)^{-3}}}}{\sqrt{1 + \frac{\kappa^2}{\sigma^6}}} , \quad (5.7)$$

$$r_{0,\pm} = \frac{\sqrt{2}q_5}{\beta^2} \frac{(1 - \Omega^2 \rho^2)^{-1} \sqrt{1 + \frac{\kappa^2}{\sigma^6}}}{\sqrt{1 \pm \sqrt{1 - \frac{4q_5^2}{\beta^6} \left(1 + \frac{\kappa^2}{\sigma^6}\right) (1 - \Omega^2 \rho^2)^{-3}}} , \quad (5.8)$$

$$\cos \theta = \frac{1}{\sqrt{1 + \frac{\kappa^2}{\sigma^6}}} . \quad (5.9)$$

Notice that the above expressions break down at the critical value

$$\sigma_b = \left(\frac{4q_2^2}{\beta^6 (1 - \Omega^2 \rho_b^2)^3 - 4q_5^2} \right)^{\frac{1}{6}} , \quad \rho_b := \rho(\sigma_b) . \quad (5.10)$$

The more explicit form of this value in the near-extremal regime will be discussed further in subsection 5.3 below.

One can show [18–20] that the remaining, extrinsic, equations for the transverse scalars can be obtained by extremizing the Dirac-like action

$$I = \frac{\Omega_{(3)} \Omega_{(4)}}{8G} L_t \int d\sigma \sqrt{1 + \rho'^2 + z'^2} F_{\pm}(\rho, \sigma) , \quad (5.11)$$

$$F_{\pm}(\rho, \sigma) = \beta^3 \sigma^3 \rho \frac{1 + 3 \sinh^2 \alpha_{\pm}}{\cosh^3 \alpha_{\pm}} (1 - \Omega^2 \rho^2)^{\frac{3}{2}} \quad (5.12)$$

where the explicit form of α_{\pm} in eq. (5.7) is implied. L_t denotes the (possibly infinite) length of the time direction. We emphasize that this action is suitable only for stationary configurations. For more generic deformations of the M2-M5 bound state one should consider directly the full blackfold equations (4.7)-(4.9).

Varying (5.11), (5.12) with respect to the unknown scalars ρ, z we obtain the equations of motion

$$\partial_{\rho} F_{\pm} \sqrt{1 + \rho'^2 + z'^2} = \left(\frac{\rho' F_{\pm}}{\sqrt{1 + \rho'^2 + z'^2}} \right)' , \quad (5.13)$$

$$\left(\frac{z' F_{\pm}}{\sqrt{1 + \rho'^2 + z'^2}} \right)' = 0. \quad (5.14)$$

Using the boundary conditions (4.16) and combining with (5.14) we can also recast (5.13) into the more convenient form

$$\left(\frac{\rho'}{z'} \right)' = z' \frac{F_{\pm} \partial_{\rho} F_{\pm}}{F_{0,\pm}^2}, \quad F_{0,\pm} := F_{\pm}(\rho(\sigma_0), \sigma_0). \quad (5.15)$$

In the next subsection we solve these complicated equations perturbatively in the small temperature limit. Once we have a solution its thermodynamic data are immediately obtainable from the following expressions

$$\frac{dM}{dz} = \frac{\Omega_{(3)} \Omega_{(4)} \beta^3}{8G} \sigma^3 \rho \sqrt{1 - \Omega^2 \rho^2} \frac{1 + 3 \cosh^2 \alpha_{\pm} - \Omega^2 \rho^2 (1 + 3 \sinh^2 \alpha_{\pm})}{\cosh^3 \alpha_{\pm}} \frac{F_{\pm}}{F_{0,\pm}}, \quad (5.16)$$

$$\frac{dJ}{dz} = \frac{3 \Omega_{(3)} \Omega_{(4)} \Omega \beta^3 \sigma^3 \rho \sqrt{1 - \Omega^2 \rho^2}}{8G \cosh^3 \alpha_{\pm}} \frac{F_{\pm}}{F_{0,\pm}}, \quad (5.17)$$

$$\frac{dS}{dz} = \frac{\pi \Omega_{(3)} \Omega_{(4)} \beta^4 \sigma^3 \rho (1 - \Omega^2 \rho^2)^{\frac{3}{2}}}{2G \cosh^3 \alpha_{\pm}} \frac{F_{\pm}}{F_{0,\pm}}. \quad (5.18)$$

5.2 Small temperature expansion

The equations of motion (5.13), (5.14) admit a perturbative small temperature ($\beta \gg 1$) expansion with

$$z(\sigma) = \sum_{n=0}^{\infty} z_n(\sigma) \beta^{-\frac{3n}{2}}, \quad \rho(\sigma) = \sum_{n=0}^{\infty} \rho_n(\sigma) \beta^{-\frac{3n}{2}}. \quad (5.19)$$

In this expansion the coefficients $\rho_n(\sigma)$ are determined order by order by algebraic equations, and $z_n(\sigma)$ by first order ODEs. Focusing on the $+$ branch that connects smoothly to the extremal solutions, we find at the first few orders

$$\rho(\sigma) = \frac{1}{\Omega} \left(1 - \frac{\sqrt{q_2} (1 + \frac{\sigma_0^6}{\kappa^2})^{\frac{1}{4}}}{\sigma^{\frac{3}{2}}} \beta^{-\frac{3}{2}} - \frac{q_2}{192 \kappa \Omega^2} \frac{9 \kappa^2 (-8 \sigma^{12} + 14 \sigma^6 \sigma_0^6 + \kappa^2 (\sigma^6 + 5 \sigma_0^6)) + 40 \sigma^2 (\kappa^2 + \sigma_0^6)^3 \Omega^2}{\sigma^5 (\kappa^2 + \sigma_0^6)^{\frac{5}{2}}} \beta^{-3} + \mathcal{O}(\beta^{-\frac{9}{2}}) \right), \quad (5.20)$$

$$z'(\sigma) = -\sqrt{\frac{\sigma_0^6 + \kappa^2}{\sigma^6 - \sigma_0^6}} + \frac{2\sqrt{q_2} (\kappa^2 + \sigma_0^6) \sqrt{\kappa^2 + \sigma_0^6}}{3\sqrt{\kappa} (\sigma^6 - \sigma_0^6)^{\frac{3}{2}}} \left[\left(1 + \frac{\kappa^2}{\sigma_0^6} \right)^{\frac{1}{4}} - \left(1 + \frac{\kappa^2}{\sigma^6} \right)^{\frac{1}{4}} \right] \beta^{-\frac{3}{2}} + \mathcal{O}(\beta^{-3}). \quad (5.21)$$

Integrating the last equation over σ with the boundary condition $\lim_{\sigma \rightarrow +\infty} z(\sigma) = 0$ we determine the precise form of the function $z(\sigma)$. Notice in (5.20) that the behavior of the functions (z'_0, z'_1) around the points $\sigma_0, +\infty$ is

$$(z'_0, z'_1) \sim \frac{1}{\sqrt{\sigma - \sigma_0}}, \quad \text{as } \sigma \rightarrow \sigma_0^+ \quad \text{and} \quad (z'_0, z'_1) \sim \frac{1}{\sigma^3}, \quad \text{as } \sigma \rightarrow +\infty. \quad (5.22)$$

Hence, the functions (z_0, z_1) converge in $[\sigma_0, +\infty)$. The analytic expression of $z_0(\sigma)$ was given in formula (4.17). For $z_1(\sigma)$ we have not been able to find a solution in closed analytic form, but one can be found numerically.

5.3 Note on characteristic scale hierarchies

So far the perturbative solutions (5.20), (5.21) have an undetermined parameter, σ_0 . In order to determine the precise form of a finite-temperature rotating spike solution σ_0 should be fixed in terms of the constant parameters T, Ω . In the next subsection we describe how this can be achieved with a prescription proposed in [28]. Before that, however, it will be useful to make a small parenthesis to note a related hierarchy of scales that characterize our setup.

In subsections 3.3 and 4.2 we discussed a characteristic radial scale $\sigma_c(N_2, N_5)$ (4.20) below which the perturbative blackfold expansion scheme breaks down. In the near-extremal regime this scale is controlled solely by the number of M2 and M5 branes, and is independent of the temperature and angular velocity T, Ω .

In subsection 5.1 we discussed another characteristic scale σ_b , (5.10), where the leading order blackfold solution breaks down. With the use of the explicit perturbative form of the function $\rho(\sigma)$ (5.20), we find that the leading order temperature dependence of σ_b is

$$\sigma_b \sim \frac{q_2^{\frac{1}{3}}}{\beta}. \quad (5.23)$$

In the next subsection we shall use the prescription of Ref. [28] to determine σ_0 . Anticipating the result, which exhibits the scaling behavior

$$\sigma_0 \sim \left(\frac{q_2}{\beta} \right)^{\frac{1}{5}}, \quad (5.24)$$

we deduce the important near-extremal hierarchy of scales

$$\sigma_b \ll \sigma_0 \ll \sigma_c \quad (5.25)$$

that was noted also in [21] for the static M2-M5 intersection. This behavior is depicted in figure 1.

5.4 Boundary conditions

The extremal spike that describes the rotating M2-M5 intersection is a solution with $\sigma_0 = 0$. Although the tip, at $\sigma_0 = 0 \ll \sigma_c$, lies well beyond the regime of validity of the blackfold expansion scheme, we have seen that the leading order computation (4.25) recovers correctly the tension and angular momentum density of the intersecting M2 branes.

It has been proposed [28] (in the context of the F1-D3 system) that the near-extremal spike solutions can be determined by requiring that they exhibit an analogous matching of thermodynamic data at a non-vanishing σ_0 controlled by the finite temperature. Again, this entails an extrapolation away from the regime of validity of the descriptions we are using whose success relies on a miraculous agreement with exact data that is not immediately obvious.

In Ref. [21] we presented favorable evidence for the applicability of this prescription to the near-extremal static M2-M5 intersection. By matching the tension and entropy density of the blackfold spike to the corresponding quantities of a static black M2 at σ_0 one obtains, as in the case of the F1-D3 system [28], two independent conditions for a single unknown. The two resulting values of σ_0 were found to agree within 4% at the leading order temperature dependence providing evidence

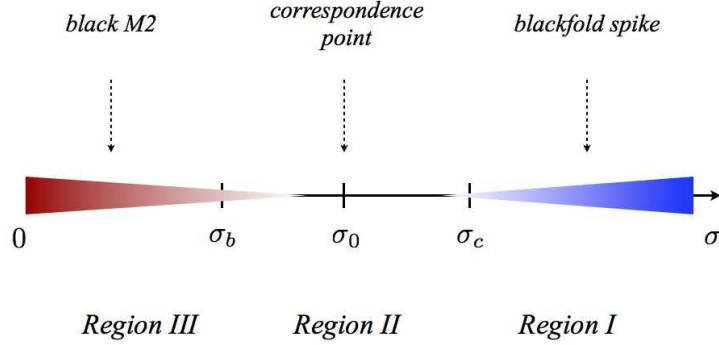


Figure 1: Three different regions (I, II, III) on the semi-infinite σ line. σ_c is the characteristic scale where the regime of validity of the leading order blackfold approximation ends. σ_b is the point where a thermal spike solution breaks down. σ_0 denotes the correspondence point where the thermodynamic data of a black M2 brane are matched to the thermodynamic data of the blackfold spike. Figure reprinted from [21].

for the consistency of the approach. Since there is no a priori justification for this rather useful prescription it is interesting to know if it is equally successful in other more generic setups. The rotating M2-M5 intersection provides a new more involved example where instead of two independent matching conditions we have four. The miracles of the extremal description imply that any deviations will be suppressed by the temperature. Hence, it is sensible to focus on the leading order temperature behavior of the solutions in the near-extremal limit.

The precise form of the matching conditions is the following

$$\left(\frac{dM}{dz} \Big|_{\sigma=\sigma_0^+} \right)_{\text{M2-M5}} = T_{M2}, \quad \left(\frac{dJ}{dz} \Big|_{\sigma=\sigma_0^+} \right)_{\text{M2-M5}} = \mathcal{J}_{M2}, \quad (5.26)$$

$$\left(\frac{dS}{dz} \Big|_{\sigma=\sigma_0^+} \right)_{\text{M2-M5}} = s_{M2}, \quad \rho(\sigma_0)_{\text{M2-M5}} = \rho_{M2} \quad (5.27)$$

where T_{M2} , \mathcal{J}_{M2} , s_{M2} and ρ_{M2} denote respectively the tension, angular momentum density, entropy density and cylinder radius of the black M2 evaluated at the same temperature, angular velocity and number of M2 branes as in the M2-M5 system. The second condition in (5.27) requires the matching of a geometric datum. Each of these conditions determines independently a specific value for σ_0 and there is no apparent reason why these values should be the same. The observed agreement or disagreement is a measure of how well the matching scheme (5.26), (5.27) works.

The matching of the two descriptions (the M2 and the deformed M5) at σ_0 is performed in an intermediate region where neither is strictly valid [28, 21]. From the extrapolated leading order M2-M5 blackfold description this implies that the matching is performed in a regime where

$$\sigma_0 \ll \sigma_c, \quad \sigma_0^6 \ll \kappa^2. \quad (5.28)$$

The first inequality declares that we are working outside the strict regime of validity of the blackfold description, and the second inequality that we are describing a region where the contribution of the M2 branes dominates. With these assumptions the small temperature expansion of the quantities appearing in (5.26), (5.27) yields the following results.

From the expansion of the tensions we find

$$\begin{aligned} \left(\frac{dM}{dz} \Big|_{\sigma=\sigma_0^+} \right)_{M2-M5} &= -\frac{4\pi Q_2}{\Omega} \left[1 - \frac{\sqrt{q_2}}{6} \left(1 + \frac{27\sigma_0^4}{4\kappa^2\Omega^2} \right) \sigma_0^{-\frac{3}{2}} \beta^{-\frac{3}{2}} + \dots \right], \\ T_{M_2} &= -\frac{4\pi Q_2}{\Omega} \left(1 - \frac{1}{3 \cdot 2^{\frac{3}{5}}} q_2^{\frac{1}{5}} \beta^{-\frac{6}{5}} + \dots \right). \end{aligned} \quad (5.29)$$

The dots denote subleading contributions in the temperature. The right hand side of the first equation includes inside the parenthesis an Ω -dependent contribution. Since we work in the limit of infinitesimal temperature and correspondingly infinitesimal σ_0 it is consistent to drop this term, *i.e.* assume $\sigma_0^4 \ll \kappa^2\Omega^2$.⁶ Then, from the first matching condition in (5.26) we obtain

$$\sigma_0^{(M)} = \left(\frac{q_2}{2^{4/3}\beta} \right)^{\frac{1}{5}} + \dots \quad (5.30)$$

We are using the superscript ^(M) to keep track of the fact that this value is obtained from (5.26) by matching the tensions.

Similarly, from the expansion of angular densities we find

$$\begin{aligned} \left(\frac{dJ}{dz} \Big|_{\sigma=\sigma_0^+} \right)_{M2-M5} &= -\frac{2\pi Q_2}{\Omega^2} \left[1 - \sqrt{q_2} \left(\frac{2}{3} + \frac{9\sigma_0^4}{4\kappa^2\Omega^2} \right) \sigma_0^{-\frac{3}{2}} \beta^{-\frac{3}{2}} + \dots \right], \\ \mathcal{J}_{M_2} &= -\frac{2\pi Q_2}{\Omega^2} \left(1 - \frac{5}{3 \cdot 2^{\frac{8}{5}}} q_2^{\frac{1}{5}} \beta^{-\frac{6}{5}} + \dots \right). \end{aligned} \quad (5.31)$$

Dropping again the $\frac{\sigma_0^4}{\kappa^2\Omega^2}$ term in the right hand side of the first equation we obtain

$$\sigma_0^{(J)} = \frac{2^{\frac{13}{5}}}{5^{\frac{2}{5}}} \left(\frac{q_2}{\beta} \right)^{\frac{1}{5}} + \dots \quad (5.32)$$

From the expansion of the entropy densities we obtain

$$\left(\frac{dS}{dz} \Big|_{\sigma=\sigma_0^+} \right)_{M2-M5} = -\frac{8\pi^2 Q_2}{3\Omega} \sqrt{q_2} \sigma_0^{-\frac{3}{2}} \beta^{-\frac{1}{2}} + \dots, \quad s_{M_2} = -\frac{4\pi^2 Q_2}{3\Omega} 2^{\frac{2}{5}} \left(\frac{q_2}{\beta} \right)^{\frac{1}{5}} + \dots \quad (5.33)$$

yielding the matching point

$$\sigma_0^{(S)} = \left(\frac{4q_2}{\beta} \right)^{\frac{1}{5}} + \dots \quad (5.34)$$

⁶In the opposite regime, $\sigma_0^4 \gg \kappa^2\Omega^2$, the matching (5.26) would give $\sigma_0 \sim \beta^{\frac{3}{25}}$ which is inconsistent with the requirement $\sigma_0 \ll \sigma_c$ in the small-temperature limit, $\beta \gg 1$, keeping Ω fixed.

Finally, from the expansion of the rotation radius we find

$$\rho(\sigma_0)_{\text{M2-M5}} = \frac{1}{\Omega} \left(1 - \frac{\sqrt{q_2}}{2} \sigma_0^{-\frac{3}{2}} \beta^{-\frac{3}{2}} + \dots \right), \quad \rho_{\text{M2}} = \frac{1}{\Omega} \left(1 - \frac{1}{2^{\frac{8}{5}}} q_2^{\frac{1}{5}} \beta^{-\frac{6}{5}} + \dots \right) \quad (5.35)$$

and the same leading order expression for the matching point $\sigma_0^{(\rho)}$ as in (5.34).

It is satisfying to verify the same scaling behavior (5.24) from all the matching conditions and the corresponding hierarchy (5.25). The numerical coefficients of the precise leading order behavior of $\sigma_0(\beta)$ are also comparable and of the same order

$$\frac{\sigma_0^{(J)}}{\sigma_0^{(M)}} = \frac{2^{\frac{17}{15}}}{5^{\frac{2}{3}}} \simeq 0.750, \quad \frac{\sigma_0^{(\rho)}}{\sigma_0^{(S)}} = 1, \quad \frac{\sigma_0^{(M)}}{\sigma_0^{(S)}} = 2^{-2/3} \simeq 0.630. \quad (5.36)$$

We observe, however, that the degree of the matching varies according to the matched quantity and is less impressive than the corresponding 4% matching in the static case [21].⁷ Presumably this is an effect of the absence of supersymmetry at zero temperature.

We can summarize our approximate construction of near-extremal rotating spikes as follows. The leading order blackfold description is fixed by determining the radial dependence of the long-distance degrees of freedom $z(\sigma)$, $\rho(\sigma)$, $r_0(\sigma)$, $\alpha(\sigma)$ and $\theta(\sigma)$ with the use of eqs. (5.7)-(5.9), and (5.20), (5.21) with

$$\sigma_0 \simeq \left(\frac{\zeta q_2}{\beta} \right)^{\frac{1}{5}} + \dots \quad (5.37)$$

ζ is an order one numerical constant that is approximately fixed by the above-described schemes.

5.5 Near-extremal thermodynamics

The star of Ref. [21] was the near-extremal entropy of the static M2-M5 intersection that gave rise to the intriguing central charge expression (1.8), or equivalently (1.10). It is interesting to repeat that computation for the above stationary M2-M5-KKW solution.

The entropy of the near-extremal spike has an infrared divergence as $\sigma \rightarrow +\infty$ that needs to be regularized (we refer the reader to Ref. [21] for additional details). A renormalized version of the entropy gives

$$\begin{aligned} S &= \frac{\Omega_{(3)} \Omega_{(4)} \pi \beta^4}{2G} \int_{\sigma_0}^{+\infty} d\sigma \sigma^3 \rho \sqrt{1+z'^2+\rho'^2} \frac{(1-\Omega^2 \rho^2)^{\frac{3}{2}}}{\cosh^3 \alpha} \\ &\simeq \frac{\pi \Omega_{(3)} \Omega_{(4)} q_5^{\frac{3}{2}}}{2G \Omega \sqrt{\beta}} \int_{\sigma_0}^{+\infty} d\sigma \frac{(\kappa^2 + \sigma^6)^{\frac{5}{4}}}{\sigma^{\frac{3}{2}} \sqrt{\sigma^6 - \sigma_0^6}} + \mathcal{O}(\beta^{-2}) \\ &\simeq \frac{\pi \Omega_{(3)} \Omega_{(4)} q_5^{\frac{3}{2}}}{2G \Omega \sqrt{\beta}} \frac{\sigma_0^4 \Gamma(\frac{1}{3}) \Gamma(\frac{5}{6})}{48 \sqrt{\pi}} {}_2F_1 \left(-\frac{5}{4}, -\frac{2}{3}, -\frac{1}{6}; -\frac{\kappa^2}{\sigma_0^6} \right) + \mathcal{O}(\beta^{-2}) \\ &\simeq \frac{\pi^{\frac{3}{2}} \Omega_{(3)} \Omega_{(4)} q_5^{\frac{3}{2}}}{G \Omega \sqrt{\beta}} \frac{\kappa^{\frac{5}{2}} \Gamma(\frac{7}{12})}{\sigma_0^{\frac{7}{2}} \Gamma(\frac{1}{12})} + \Omega(\beta^{-2}). \end{aligned} \quad (5.38)$$

⁷The apparent exact agreement between $\sigma_0^{(\rho)}$ and $\sigma_0^{(S)}$ is curious. We do not have a clear understanding of this fact.

In the last equality we picked the first term in the expansion $\sigma_0 \ll \kappa^{\frac{1}{3}}$. Substituting the leading order expression (5.37) for σ_0 we find (up to an overall numerical coefficient)

$$S \sim \frac{1}{G} \frac{q_2^{\frac{9}{5}} \beta^{\frac{1}{5}}}{\Omega q_5} \quad (5.39)$$

which diverges in the zero temperature limit. Clearly, there is an important exchange of limits issue here where taking the zero temperature limit first and then doing the integral gives a different result from doing the integral first and then taking the zero temperature limit.

An analogous computation of the angular momentum of the solution gives

$$\begin{aligned} J &= \frac{3\Omega_{(3)}\Omega_{(4)}\Omega\beta^3}{8G} \int_{\sigma_0}^{+\infty} d\sigma \sigma^3 \rho^3 \sqrt{1+z'^2+\rho'^2} \frac{\sqrt{1-\Omega^2\rho^2}}{\cosh^3\alpha} \\ &\simeq \frac{3\Omega_{(3)}\Omega_{(4)}q_5}{8G\Omega^2} \int_{\sigma_0}^{+\infty} d\sigma \frac{\kappa^2 + \sigma^6}{\sqrt{\sigma^6 - \sigma_0^6}} + \mathcal{O}(\beta^{-\frac{3}{2}}) \\ &\simeq \frac{\Omega_{(3)}\Omega_{(4)}q_5}{G\Omega^2} \frac{\sigma_0^4 \Gamma(1/3)\Gamma(5/6)}{128\sqrt{\pi}} \left(1 + \frac{4\kappa^2}{\sigma_0^6}\right) + \mathcal{O}(\beta^{-\frac{3}{2}}) \\ &\simeq \frac{\Omega_{(3)}\Omega_{(4)}q_5}{G\Omega^2} \frac{\kappa^2}{\sigma_0^2} \frac{\Gamma(1/3)\Gamma(5/6)}{32\sqrt{\pi}} + \mathcal{O}(\beta^{-\frac{3}{2}}). \end{aligned} \quad (5.40)$$

In the last equality we picked again the first term in the expansion $\sigma_0 \ll \kappa^{\frac{1}{3}}$.

Combining the two expressions (5.38) and (5.40) we find a particularly simple expression for the entropy

$$S \simeq \frac{32\pi^{\frac{1}{4}}}{\sqrt{6}\zeta} \frac{\Gamma(\frac{7}{12})}{\Gamma(\frac{1}{12})\sqrt{\Gamma(\frac{1}{6})\Gamma(\frac{1}{3})}} \sqrt{\frac{N_2^2 J}{N_5}} + \dots \quad (5.41)$$

Although this is the expression for the entropy of a *near-extremal* black hole, the leading term is reminiscent of the Bekenstein-Hawking entropy of an extremal rotating BTZ black hole

$$S_{\text{BTZ}} = 2\pi \sqrt{\frac{c_{\text{BTZ}} J}{6}} \quad (5.42)$$

for a dual CFT with central charge $c_L = c_R = c_{\text{BTZ}}$. A naive comparison with eq. (5.41) gives

$$c_{\text{BTZ}} \simeq \{0.014, 0.436, 0.578\} \frac{N_2^2}{N_5} \quad (5.43)$$

where each of the three numerical coefficients corresponds to ζ obtained respectively from the matching scheme based on the entropy, mass and angular momentum densities. We observe that the (N_2, N_5) scaling of this expression is exactly the same as the one deduced in [21] from the static M2-M5 intersection (1.10). It is amusing that even the numerical coefficient (~ 0.6 in (1.10)) is comparable with the above coefficients—especially the third one based on the matching of angular momentum densities in (5.32).

This agreement may be sensible since both in the static and stationary cases we are probing the same two-dimensional superconformal field theory at the orthogonal M2-M5 intersection in

different states. Presumably, in the static case we are probing a ground state with vanishing left-right scaling dimensions, whereas in the stationary rotating case we are probing a state with the left-moving sector in an excited state. Despite these expectations, there is a lot that remains to be understood about the validity of the overall picture, the precise physical interpretation of (5.41) and the intriguing agreements between (5.43) and (1.10). We comment further on this aspect in the next concluding section.

6. Open problems

In Refs. [20, 21] and the above presentation we discussed the leading order effective field theory description of fully localized orthogonal M2-M5 intersections. It should be appreciated that the exact supergravity solutions of these systems (both extremal and non-extremal) are not known and therefore the effective descriptions of this work are opening the route to a new more efficient treatment. One of the primary ultimate goals in this application to the M2-M5 system is the identification of the two-dimensional $\mathcal{N} = (4, 4)$ SCFT at the intersection by means of holography and its implications for the microscopic structure of the M5 brane in M-theory. Preliminary results like the formulae (1.8) are indicative of a rich underlying structure that remains to be explored.

In much of this report we described the assumptions, limitations, but also unexpected merits of a leading order effective field theory treatment of the intersection. An important part of the story, and the natural next step in the analysis we have performed, is the development of the precise map between a solution of the hydrodynamic effective blackfold theory and the corresponding bulk supergravity solution. Much like in the fluid-gravity correspondence it is expected that this map is one-to-one. Considerable progress has been achieved in proving this fact in the fluid-gravity version of the AdS/CFT correspondence, however it remains a largely open and rather involved technical problem in the case of general blackfolds. So far the state-of-the-art in this direction has been achieved in non-supersymmetric pure gravity contexts [42, 24, 44]. Further technical progress in general supergravity theories appears to be most imminent for extremal configurations [45].

For the M2-M5 system, which is the system of interest in this work, a direct reconstruction of the bulk supergravity solution will be useful for several reasons, some of which can be summarized as follows:

- For static 1/4-BPS configurations it will allow to make contact with the exact solution generating techniques of Ref. [16]. Identifying the near-horizon geometry will be a big step forward in developing the AdS_3/CFT_2 correspondence of this system and verifying the validity of the central charge expressions (1.8). In particular, it will allow us to verify the applicability of the general central charge formula (1.2) and determine the precise relation between the integers k_+ , k_- and the number of M2 and M5 branes N_2, N_5 respectively. It is also interesting to explore whether the new expansion in powers of $\frac{1}{\lambda}$ (see eq. (1.5)) simplifies this analysis and takes us one step further compared to previous work. In addition, knowledge of the exact supergravity solution will help clarify the convergence properties of the perturbative blackfold expansion scheme and the miraculous agreements observed in Ref. [20].

- The corresponding analysis of the extremal non-supersymmetric orthogonal M2-M5-KKW intersection will help clarify analogous questions in a non-supersymmetric setting, in particular the mysteries of section 5.5.
- More generally, the development of a precise one-to-one map between effective hydrodynamic solutions and supergravity backgrounds will be very useful in clarifying the potential holographic nature of such maps where one links a supergravity solution to an effective hydrodynamic (blackfold) solution to a microscopic state of the underlying brane system. This is potentially a promising new route towards a much more general understanding of holography beyond the near-horizon limit and anti-deSitter spaces. The recent work [46] is based on a related logic.

We hope to return with a detailed discussion of these issues in future work.

Acknowledgements

We would like to thank Jan de Boer, Jerome Gauntlett, Elias Kiritsis, Niels Obers, Kostas Skenderis and Arkady Tseytlin for useful comments on the literature and inspiring discussions. The research of VN was in part supported by grants PERG07-GA-2010-268246, and the EU program ‘‘Thales’’ ESF/NSRF 2007-2013. It was also co-financed by the European Union (European Social Fund, ESF) and Greek national funds through the Operational Program ‘‘Education and Lifelong Learning’’ of the National Strategic Reference Framework (NSRF) under ‘‘Funding of proposals that have received a positive evaluation in the 3rd and 4th Call of ERC Grant Schemes’’. The research of KS has been supported by an ARC contract No. AUWB-2010-10/15-UMONS-1, a Fund for Scientific Research-FNRS (Belgium), by IISN-Belgium (convention 4.4511.06), by ‘‘Communauté française de Belgique - Actions de Recherche Concertées’’, the ITN programme PITN-GA-2009-237920, the ERC Advanced Grant 226371, the IFCPAR CEFIPRA programme 4104-2 and the ANR programme blanc NT09-573739. KS would like also to thank the University of Patras and the University of Crete for hospitality where part of this work was done.

A. Thermodynamics of stationary M2 brane cylinders

For quick reference in this appendix we list the properties of a rotating M2 black cylinder.

We consider an M2 black brane in flat space parametrized in cylindrical coordinates as

$$ds^2 = -dt^2 + \rho^2 d\theta^2 + d\rho^2 + dz^2 + \sum_{i=1}^7 (dx^i)^2 . \quad (\text{A.1})$$

The M2 brane is oriented along the directions (t, θ, z) and rotates along the angular θ direction with velocity vector

$$u = \frac{1}{\sqrt{1 - \Omega^2 \rho^2}} \left(\frac{\partial}{\partial t} + \Omega \frac{\partial}{\partial \theta} \right) . \quad (\text{A.2})$$

The relevant thermodynamic quantities

$$\varepsilon = \frac{\Omega_{(7)}}{16\pi G} r_0^6 (1 + 6 \cosh^2 \alpha) , \quad \mathcal{F} = \frac{3}{2\pi r_0 \cosh \alpha} , \quad s = \frac{\Omega_{(7)}}{4G} r_0^7 \cosh \alpha , \quad (\text{A.3})$$

$$Q_2 = -\frac{\Omega^{(7)}}{16\pi G} 6r_0^6 \sinh \alpha \cosh \alpha, \quad \Phi_2 = -\tanh \alpha \quad (\text{A.4})$$

imply the stress-energy tensor

$$T_{ab} = \mathcal{F} s \left(u_a u_b - \frac{1}{6} \gamma_{ab} \right) - \Phi_2 Q_2 \gamma_{ab}. \quad (\text{A.5})$$

At equilibrium the unknown worldvolume functions r_0, α, ρ can be determined in terms of the constants T, Q_2, Ω using the equations

$$\tilde{q}_2 = -\frac{16\pi G}{6\Omega^{(7)}} Q_2 = r_0^6 \sinh \alpha \cosh \alpha, \quad (\text{A.6})$$

$$r_0 \cosh \alpha = \sqrt{1 - \Omega^2 \rho^2} \tilde{\beta}, \quad \tilde{\beta} := \frac{3}{2\pi T}, \quad (\text{A.7})$$

$$\Omega^2 \rho^2 = \frac{1 + 6 \sinh^2 \alpha}{1 + 6 \cosh^2 \alpha}. \quad (\text{A.8})$$

Comparing (A.6), (A.7) with (5.4),(5.6) we can easily find that $(\tilde{q}_2, \tilde{\beta}) = (8q_2, 2\beta)$. Notice that (A.8) is consistent with equation (3.6) of [19] for $p = 1$ and it can be also derived by requiring $T^{11} = 0$. It is useful to rewrite eqs. (A.6), (A.7) as

$$r_0 = \left(\frac{\tilde{q}_2}{\sinh \alpha \cosh \alpha} \right)^{1/6}, \quad \tilde{\beta} = \cosh \alpha \left(\frac{\tilde{q}_2}{\sinh \alpha \cosh \alpha} \right)^{1/6} \sqrt{\frac{1 + 6 \cosh^2 \alpha}{6}} \quad (\text{A.9})$$

where use was made of (A.8).

Accordingly, the thermodynamics of the general non-extremal cylinder solution is

$$M = -\frac{4\pi Q_2}{3\Omega} L_z \sqrt{\frac{1 + 6 \sinh^2 \alpha}{1 + 6 \cosh^2 \alpha}} \frac{2 + 3 \sinh^2 \alpha}{\sinh \alpha \cosh \alpha}, \quad (\text{A.10})$$

$$J = -\frac{\pi Q_2}{3\Omega^2} L_z \frac{(1 + 6 \sinh^2 \alpha)^{3/2}}{\sqrt{1 + 6 \cosh^2 \alpha}} \frac{1}{\sinh \alpha \cosh \alpha}, \quad (\text{A.11})$$

$$S = -\frac{(2\pi)^2 Q_2}{3\Omega} L_z r_0 \sqrt{\frac{1 + 6 \sinh^2 \alpha}{1 + 6 \cosh^2 \alpha}} \frac{\tilde{\beta}}{\sinh \alpha \cosh \alpha} \quad (\text{A.12})$$

In the extremal limit, where (Q_2, Ω) are kept fixed, eqs. (A.8), (A.9) imply

$$\tilde{\beta} \rightarrow \infty, \quad \alpha \rightarrow \infty, \quad r_0 \rightarrow 0, \quad \rho = \frac{1}{\Omega}. \quad (\text{A.13})$$

Moreover, using the definition (4.1) one can check that the null momentum density is

$$\mathcal{H} = |Q_2| \quad (\text{A.14})$$

and the rest of the thermodynamics becomes

$$\frac{M}{L_z} = -\frac{4\pi Q_2}{\Omega}, \quad \frac{J}{L_z} = -\frac{2\pi Q_2}{\Omega^2}, \quad \frac{S}{L_z} = -\frac{(2\pi)^2 Q_2}{3\Omega} r_0 \rightarrow 0. \quad (\text{A.15})$$

Away from extremality we have to solve (A.9) for non-zero temperatures. This can be done easily with a perturbative expansion

$$\cosh \alpha = y^{3/5} - \frac{1}{10y^{3/5}} - \frac{43}{1200y^{9/5}} - \frac{137}{4320y^3} + \mathcal{O}(y^{-21/5}), \quad y := \frac{\tilde{\beta}}{\tilde{q}_2^{1/6}} \quad (\text{A.16})$$

around extremality. Plugging this expansion into the expressions (A.8), (A.10), (A.11), (A.12) we find respectively

$$\begin{aligned} \rho &\simeq \frac{1}{\Omega} \left(1 - \frac{\tilde{q}_2^{1/5}}{2\tilde{\beta}^{6/5}} - \frac{17\tilde{q}_2^{2/5}}{120\tilde{\beta}^{12/5}} + \mathcal{O}(y^{-18/5}) \right), \\ M &\simeq -\frac{4\pi Q_2}{\Omega} L_z \left(1 - \frac{\tilde{q}_2^{1/5}}{3\tilde{\beta}^{6/5}} + \frac{\tilde{q}_2^{2/5}}{60\tilde{\beta}^{12/5}} + \mathcal{O}(y^{-18/5}) \right), \\ J &\simeq -\frac{2\pi Q_2}{\Omega^2} L_z \left(1 - \frac{5\tilde{q}_2^{1/5}}{6\tilde{\beta}^{6/5}} - \frac{\tilde{q}_2^{2/5}}{12\tilde{\beta}^{12/5}} + \mathcal{O}(y^{-18/5}) \right), \\ S &\simeq -\frac{(2\pi)^2 Q_2}{3\Omega} L_z \left(\frac{\tilde{q}_2^{1/5}}{\tilde{\beta}^{1/5}} + \frac{\tilde{q}_2^{2/5}}{5\tilde{\beta}^{7/5}} + \frac{37\tilde{q}_2^{3/5}}{200\tilde{\beta}^{13/5}} + \mathcal{O}(y^{-23/5}) \right). \end{aligned} \quad (\text{A.17})$$

B. Extrinsic curvature and stress-energy tensors

In this appendix we provide the expressions of the extrinsic curvature and stress-energy tensors that are relevant for sections 4 and 5.

The extrinsic curvature of the embedding (3.8) can be found easily with the use of equation (A.20) in [18]. The non-vanishing components take the form

$$\begin{aligned} K_{11}^z &= \frac{\rho z' \rho'}{1+z'^2+\rho'^2}, \quad K_{22}^z = \frac{(1+\rho'^2)z'' - \rho' z' \rho''}{1+z'^2+\rho'^2}, \quad K_{33}^z = \frac{\sigma z'}{1+z'^2+\rho'^2}, \quad K_{44}^z = \frac{\sigma z' \sin^2 \psi}{1+z'^2+\rho'^2}, \\ K_{11}^\rho &= -\frac{\rho(1+z'^2)}{1+z'^2+\rho'^2}, \quad K_{22}^\rho = \frac{(1+z'^2)\rho'' - \rho' z' z''}{1+z'^2+\rho'^2}, \quad K_{33}^\rho = \frac{\sigma \rho'}{1+z'^2+\rho'^2}, \quad K_{44}^\rho = \frac{\sigma \rho' \sin^2 \psi}{1+z'^2+\rho'^2}, \\ K_{11}^r &= \frac{\rho \rho'}{1+z'^2+\rho'^2}, \quad K_{22}^r = -\frac{z' z'' + \rho' \rho''}{1+z'^2+\rho'^2}, \quad K_{33}^r = -\sigma \frac{z'^2 + \rho'^2}{1+z'^2+\rho'^2}, \quad K_{44}^r = -\sigma \sin^2 \psi \frac{z'^2 + \rho'^2}{1+z'^2+\rho'^2}, \\ K_{55}^z &= \frac{\sigma z' \sin^2 \psi \sin^2 \phi}{1+z'^2+\rho'^2}, \quad K_{55}^\rho = \frac{\sigma \rho' \sin^2 \psi \sin^2 \phi}{1+z'^2+\rho'^2}, \quad K_{55}^r = -\sigma \sin^2 \psi \sin^2 \phi \frac{z'^2 + \rho'^2}{1+z'^2+\rho'^2}, \end{aligned} \quad (\text{B.1})$$

Accordingly the mean curvature vector $K^\mu = \gamma^{ab} K_{ab}^\mu$ has three non-vanishing components

$$\begin{aligned} K^r &= \frac{\rho'}{\rho(1+z'^2+\rho'^2)} - \frac{z' z'' + \rho' \rho''}{(1+z'^2+\rho'^2)^2} - \frac{3(z'^2 + \rho'^2)}{\sigma(1+z'^2+\rho'^2)}, \\ K^z &= \frac{z' \rho'}{\rho(1+z'^2+\rho'^2)} + \frac{(1+\rho'^2)z'' - \rho' z' \rho''}{(1+z'^2+\rho'^2)^2} + \frac{3z'}{\sigma(1+z'^2+\rho'^2)}, \\ K^\rho &= -\frac{1+z'^2}{\rho(1+z'^2+\rho'^2)} + \frac{(1+z'^2)\rho'' - \rho' z' z''}{(1+z'^2+\rho'^2)^2} + \frac{3\rho'}{\sigma(1+z'^2+\rho'^2)}. \end{aligned} \quad (\text{B.2})$$

Characteristic curvature sizes of a configuration can be defined as $L_{\text{curv}}^{(i)} = |K_{(i)}|^{-1}$ with $K_{(i)} = K^\mu n^{(i)}_\mu$. $n^{(i)}_\mu$, $i = z, \rho$, are the unit normal vectors of the embedding surface of the fivebrane, $z = z(\sigma)$, $\rho = \rho(\sigma)$ respectively,

$$n^{(z)}_\mu = \frac{1}{\sqrt{1+z'^2}} (\vec{0}_2, -z', \vec{0}_3, 1, \vec{0}_4), \quad n^{(\rho)}_\mu = \frac{1}{\sqrt{1+\rho'^2}} (\vec{0}_2, -\rho', \vec{0}_4, 1, \vec{0}_3). \quad (\text{B.3})$$

After some algebra we compute the principal curvatures

$$K_{(z)} = \frac{1}{\sqrt{1+z'^2}} \left(\frac{z''}{1+z'^2+\rho'^2} + \frac{3z'}{\sigma} \right), \quad K_{(\rho)} = \frac{1}{\sqrt{1+\rho'^2}} \left(\frac{\rho''}{1+z'^2+\rho'^2} + \frac{3\rho'}{\sigma} - \frac{1}{\rho} \right). \quad (\text{B.4})$$

The mean curvature equals the half of the sum of the principal curvatures.

Finally, the stress-energy tensor (2.13) that enters into the extrinsic equations of motion (2.17) and the thermodynamics of the solution (2.19), has the non-vanishing components

$$\begin{aligned} T^{00} &= \frac{\mathcal{J}}{1-\Omega^2\rho^2} (1 + 3\cosh^2\alpha - \Omega^2\rho^2(1 + 3\sinh^2\alpha)), \\ T^{11} &= -\frac{\mathcal{J}(1 + 3\sinh^2\alpha)}{\rho^2} + \mathcal{J} \frac{3\Omega^2}{1-\Omega^2\rho^2}, \quad T^{22} = -\gamma^{22} \mathcal{J} (1 + 3\sinh^2\alpha), \\ T^{33} &= -\gamma^{33} \mathcal{J} \mathcal{J}, \quad T^{44} = -\gamma^{44} \mathcal{J} \mathcal{J}, \quad T^{55} = -\gamma^{55} \mathcal{J} \mathcal{J}, \quad T^{01} = T^{10} = \mathcal{J} \frac{3\Omega}{1-\Omega^2\rho^2}, \end{aligned} \quad (\text{B.5})$$

where

$$\mathcal{J} := \frac{r_0^3 \Omega_{(4)}}{16\pi G}, \quad \mathcal{J} := 1 + 3\cos^2\theta \sinh^2\alpha. \quad (\text{B.6})$$

References

- [1] J. Bagger and N. Lambert, ‘‘Gauge symmetry and supersymmetry of multiple M2-branes,’’ *Phys. Rev. D* **77**, 065008 (2008) [arXiv:0711.0955 [hep-th]].
- [2] A. Gustavsson, ‘‘Algebraic structures on parallel M2-branes,’’ *Nucl. Phys. B* **811**, 66 (2009) [arXiv:0709.1260 [hep-th]].
- [3] O. Aharony, O. Bergman, D. L. Jafferis and J. Maldacena, ‘‘ $\mathcal{N} = 6$ superconformal Chern-Simons-matter theories, M2-branes and their gravity duals,’’ *JHEP* **0810**, 091 (2008) [arXiv:0806.1218 [hep-th]].
- [4] A. Sevrin, W. Troost and A. Van Proeyen, ‘‘Superconformal Algebras in Two-Dimensions with $\mathcal{N} = 4$,’’ *Phys. Lett. B* **208**, 447 (1988).
- [5] J. de Boer, A. Pasquinucci and K. Skenderis, ‘‘AdS / CFT dualities involving large 2-D $\mathcal{N}=4$ superconformal symmetry,’’ *Adv. Theor. Math. Phys.* **3**, 577 (1999) [hep-th/9904073].
- [6] S. Gukov, E. Martinec, G. W. Moore and A. Strominger, ‘‘The Search for a holographic dual to $AdS_3 \times S^3 \times S^3 \times S^1$,’’ *Adv. Theor. Math. Phys.* **9**, 435 (2005) [hep-th/0403090].
- [7] P. S. Howe, N. D. Lambert and P. C. West, ‘‘The Selfdual string soliton,’’ *Nucl. Phys. B* **515**, 203 (1998) [hep-th/9709014].
- [8] P. S. Howe, E. Sezgin and P. C. West, ‘‘Covariant field equations of the M theory five-brane,’’ *Phys. Lett. B* **399**, 49 (1997) [hep-th/9702008].
- [9] I. A. Bandos, K. Lechner, A. Nurmagambetov, P. Pasti, D. P. Sorokin and M. Tonin, *Phys. Rev. Lett.* **78** (1997) 4332 [hep-th/9701149].
- [10] M. Aganagic, J. Park, C. Popescu and J. H. Schwarz, *Nucl. Phys. B* **496**, 191 (1997) [hep-th/9701166].
- [11] C. G. Callan and J. M. Maldacena, ‘‘Brane death and dynamics from the Born-Infeld action,’’ *Nucl. Phys. B* **513**, 198 (1998) [hep-th/9708147].

- [12] M. J. Duff, S. Ferrara, R. R. Khuri and J. Rahmfeld, “Supersymmetry and dual string solitons,” *Phys. Lett. B* **356**, 479 (1995) [hep-th/9506057].
- [13] A. A. Tseytlin, “Extreme dyonic black holes in string theory,” *Mod. Phys. Lett. A* **11**, 689 (1996) [hep-th/9601177].
- [14] J. P. Gauntlett, “Intersecting branes,” In *Seoul/Sokcho 1997, Dualities in gauge and string theories* 146-193 [hep-th/9705011].
- [15] D. J. Smith, “Intersecting brane solutions in string and M theory,” *Class. Quant. Grav.* **20**, R233 (2003) [hep-th/0210157].
- [16] O. Lunin, “Strings ending on branes from supergravity,” *JHEP* **0709**, 093 (2007) [arXiv:0706.3396 [hep-th]].
- [17] R. Emparan, T. Harmark, V. Niarchos and N. A. Obers, “World-Volume Effective Theory for Higher-Dimensional Black Holes,” *Phys. Rev. Lett.* **102**, 191301 (2009) [arXiv:0902.0427 [hep-th]].
- [18] R. Emparan, T. Harmark, V. Niarchos and N. A. Obers, “Essentials of Blackfold Dynamics,” *JHEP* **1003**, 063 (2010) [arXiv:0910.1601 [hep-th]].
- [19] R. Emparan, T. Harmark, V. Niarchos and N. A. Obers, “Blackfolds in Supergravity and String Theory,” *JHEP* **1108**, 154 (2011) [arXiv:1106.4428 [hep-th]].
- [20] V. Niarchos and K. Siampos, “M2-M5 blackfold funnels,” *JHEP* **1206**, 175 (2012) [arXiv:1205.1535 [hep-th]].
- [21] V. Niarchos and K. Siampos, “Entropy of the self-dual string soliton,” *JHEP* **1207**, 134 (2012) [arXiv:1206.2935 [hep-th]].
- [22] R. Emparan, T. Harmark, V. Niarchos and N. A. Obers, “Blackfold approach for higher-dimensional black holes,” *Acta Phys. Polon. B* **40**, 3459 (2009).
- [23] R. Emparan, “Blackfolds,” 8th chapter of *Black Holes in Higher Dimensions* (editor: G. Horowitz), Cambridge University Press. [arXiv:1106.2021 [hep-th]].
- [24] R. Emparan, T. Harmark, V. Niarchos and N. A. Obers, “New Horizons for Black Holes and Branes,” *JHEP* **1004**, 046 (2010) [arXiv:0912.2352 [hep-th]].
- [25] J. Camps, R. Emparan and N. Haddad, “Black Brane Viscosity and the Gregory-Laflamme Instability,” *JHEP* **1005**, 042 (2010) [arXiv:1003.3636 [hep-th]].
- [26] M. M. Caldarelli, R. Emparan and B. Van Pol, “Higher-dimensional Rotating Charged Black Holes,” *JHEP* **1104**, 013 (2011) [arXiv:1012.4517 [hep-th]].
- [27] G. Grignani, T. Harmark, A. Marini, N. A. Obers and M. Orselli, “Heating up the BIon,” *JHEP* **1106**, 058 (2011) [arXiv:1012.1494 [hep-th]].
- [28] G. Grignani, T. Harmark, A. Marini, N. A. Obers and M. Orselli, “Thermodynamics of the hot BIon,” *Nucl. Phys. B* **851**, 462 (2011) [arXiv:1101.1297 [hep-th]].
- [29] G. Grignani, T. Harmark, A. Marini, N. A. Obers and M. Orselli, “Thermal string probes in AdS and finite temperature Wilson loops,” *JHEP* **1206**, 144 (2012) [arXiv:1201.4862 [hep-th]].
- [30] J. M. Izquierdo, N. D. Lambert, G. Papadopoulos and P. K. Townsend, “Dyonic membranes,” *Nucl. Phys. B* **460**, 560 (1996) [hep-th/9508177].
- [31] M. S. Costa, “Black composite M-branes,” *Nucl. Phys. B* **495**, 195 (1997) [hep-th/9610138].

- [32] J. G. Russo and A. A. Tseytlin, “Waves, boosted branes and BPS states in m theory,” Nucl. Phys. B **490**, 121 (1997) [hep-th/9611047].
- [33] T. Harmark and N. A. Obers, “Phase structure of noncommutative field theories and spinning brane bound states,” JHEP **0003**, 024 (2000) [hep-th/9911169].
- [34] T. Harmark, “Open branes in space-time noncommutative little string theory,” Nucl. Phys. B **593**, 76 (2001) [hep-th/0007147].
- [35] A. A. Tseytlin, “Harmonic superpositions of M-branes,” Nucl. Phys. B **475**, 149 (1996) [hep-th/9604035].
- [36] N. Ohta and T. Shimizu, “Nonextreme black holes from intersecting M-branes,” Int. J. Mod. Phys. A **13**, 1305 (1998) [hep-th/9701095].
- [37] S. Bhattacharyya, V. E. Hubeny, S. Minwalla and M. Rangamani, “Nonlinear Fluid Dynamics from Gravity,” JHEP **0802**, 045 (2008) [arXiv:0712.2456 [hep-th]].
- [38] V. E. Hubeny, S. Minwalla and M. Rangamani, “The fluid/gravity correspondence,” arXiv:1107.5780 [hep-th].
- [39] B. Carter, “Essentials of classical brane dynamics,” Int. J. Theor. Phys. **40**, 2099 (2001) [gr-qc/0012036].
- [40] M. M. Caldarelli, R. Emparan and M. J. Rodriguez, “Black Rings in (Anti)-deSitter space,” JHEP **0811**, 011 (2008) [arXiv:0806.1954 [hep-th]].
- [41] J. Armas and N. A. Obers, “Blackfolds in (Anti)-de Sitter Backgrounds,” Phys. Rev. D **83**, 084039 (2011) [arXiv:1012.5081 [hep-th]].
- [42] R. Emparan, T. Harmark, V. Niarchos, N. A. Obers and M. J. Rodriguez, “The Phase Structure of Higher-Dimensional Black Rings and Black Holes,” JHEP **0710**, 110 (2007) [arXiv:0708.2181 [hep-th]].
- [43] I. R. Klebanov and A. A. Tseytlin, “Entropy of near extremal black p-branes,” Nucl. Phys. B **475**, 164 (1996) [hep-th/9604089].
- [44] J. Camps and R. Emparan, “Derivation of the blackfold effective theory,” JHEP **1203**, 038 (2012) [Erratum-ibid. **1206**, 155 (2012)] [arXiv:1201.3506 [hep-th]].
- [45] V. Niarchos and K. Siampos, work in progress.
- [46] M. M. Caldarelli, J. Camps, B. Gouteraux and K. Skenderis, “AdS/Ricci-flat correspondence and the Gregory-Laflamme instability,” [arXiv:1211.2815 [hep-th]].